Design Optimization of Single-Layer Antireflective Coating for GaAs[subscript 1−x]xP[subscript x]x/ Si Tandem Cells With x=0, 0.17, 0.29, and 0.37

Citation: Abdul Hadi, Sabina, Tim Milakovich, Mayank T. Bulsara, Sueda Saylan, Marcus S. Dahlem, Eugene A. Fitzgerald, and Ammar Nayfeh. "Design Optimization of Single-Layer Antireflective Coating for GaAs[subscript 1−x]xP[subscript x]x/Si Tandem Cells With x=0, 0.17, 0.29, and 0.37." IEEE J. Photovoltaics 5, no. 1 (January 2015): 425–431.

As Published: http://dx.doi.org/10.1109/JPHOTOV.2014.2363559

Publisher: Institute of Electrical and Electronics Engineers (IEEE)

Persistent URL: http://hdl.handle.net/1721.1/108586

Version: Author's final manuscript: final author's manuscript post peer review, without publisher's formatting or copy editing

Design Optimization of Single Layer Anti-Reflective Coating for $GaAs_{1-x}P_x$ / Si Tandem Cells with x = 0, 0.17, 0.29 and 0.37

Sabina Abdul Hadi, Tim Milakovich, Mayank T. Bulsara, Sueda Saylan, Marcus S. Dahlem,
Eugene A. Fitzgerald and Ammar Nayfeh

***Abstract*—Single layer anti-reflective coating (SLARC) materials and design for $GaAs_{1-x}P_x$/Si tandem cells were analyzed by TCAD simulation. We have shown that optimum SLARC thickness is a function of bandgap, thickness and material quality of top $GaAs_{1-x}P_x$ subcell. Cells are analyzed for P fractions x=0, 0.17, 0.29 and 0.37 and ARC materials: Si_3N_4, SiO_2, ITO, HfO_2 and Al_2O_3. Optimum ARC thickness ranges from 65-75 nm for Si_3N_4 and ITO to ~100-110 nm for SiO_2. Optimum ARC thickness increases with increasing $GaAs_{1-x}P_x$ absorber layer thickness and with decreasing P fraction x. Simulations show that optimum $GaAs_{1-x}P_x$ absorber layer thickness is not a strong function of ARC material, but it increases from 250 nm for x= 0 to ~1 µm for x= 0.29 and 0.37. For all P fractions, Si_3N_4, HfO_2 and Al_2O_3 performed almost equally, while SiO_2 and ITO resulted in ~1% and ~2% lower efficiency, respectively. Optimum SLARC thickness increases as material quality of the top cell increases. The effect of ARC material decreases with decreasing $GaAs_{1-x}P_x$ material quality. The maximum efficiencies are achieved for cells with ~1 µm $GaAs_{0.71}P_{0.29}$ absorber (τ=10 ns): ~26.57% for 75 nm Si_3N_4 SLARC and 27.62% for 75 nm SiO_2/60 nm Si3N4 double layer ARC.**

***Index Terms*— Anti-reflective coating, $GaAs_{1-x}P_x$, III-V on Si, Si_3N_4, ITO, SiO_2, Al_2O_3, HfO_2, Synopsys, TCAD, TMM.**

I. INTRODUCTION

PERFORMANCE of solar cells can be greatly improved with optimized anti-reflective coating (ARC) that reduces amount of reflected incident light. Uncoated crystalline silicon (c-Si) surface (refractive index n~3.7) at interface with air (n~1) is shown to reflect between 31% - 48% of incident light [1]. The concepts of optimum ARC material, number of layers, layer thickness and surface texturing are continually being studied [1 - 7]. Ideally, the ARC should be abundant material, easily deposited, transparent to most of the solar spectrum and compatible with materials and processes commonly used in solar cell industry.

Single layer ARC (SLARC) can minimize reflection at one specific wavelength (quarter-wave ARC). However, the remaining part of the solar spectrum is highly reflected. Hence, for optimum solar cell operation, SLARC is used to minimize wavelength with highest spectral intensity. Double and multilayer anti-reflective coatings can minimize reflection for more than one wavelength of interest, but the choice of the ARC materials is more constricted, due to refractive index constraints [2-4]. Different materials such as SiO_2, SiO_x, SiN_x, Si_3N_4, ZnO, ZnS, ITO, TiO_2, MgF_2/ZnS, etc. have been shown to have good ARC properties [1-7], but their performance depends on ARC design and solar cell application. Furthermore, reflectance can be greatly reduced by surface patterning, which is of most interest for concentrated solar cells with normal light incidence [2].

With growing development of tandem cell applications for high efficiency, ARC design specifically tuned to optimize multijunction (MJ) cell performance is needed. Subcells can be grown on top of each other or they can be fabricated separately and mechanically bonded. Theoretically, optimal efficiency of two junction solar cell can be achieved if bottom cell bandgap, E_g, is 1.1 eV, while bandgap of top cell is 1.7 eV [8]. Therefore Si (E_g=1.12 eV) based tandem cells with top $GaAs_{1-x}P_x$ cell (E_g=1.42 - 2.22 eV for x = 0 - 1) are an attractive area of research for low cost MJ solar cells.

Main challenges for $GaAs_{1-x}P_x$ / Si tandem cell are lattice and thermal expansion mismatch between Si and $GaAs_{1-x}P_x$ compounds. Nonetheless, high-quality GaAs solar cells were successfully grown on Si by using SiGe step-graded buffers in order to grow virtual Ge substrate that is latticed matched to GaAs [9, 10]. Furthermore, Ge fraction in step-graded buffers can be tuned to lattice match desired $GaAs_{1-x}P_x$ compound [11, 12]. Unfortunately, due to its optical properties and decreasing bandgap, SiGe buffer layer would absorb light intended for bottom Si cell [13-15]. Another successful way to grow a defect-free III-V layer on silicon is based on the use of a GaP nucleation layer, followed by $GaAs_{1-x}P_x$ graded buffer [16-19]. The method that would avoid use of graded buffer layers and its related optical losses is mechanical stacking of two sub-cells. In this work we present simulation of the structure that represents mechanically bonded $GaAs_{1-x}P_x$ and Si cells.

For optimum performance of MJ cells, current generated in all sub-cells need to match. Sub-cell with lowest optically

---

Date Submitted: July, 22nd, 2014.

This work was supported by Masdar Institute of Science and Technology (MIST), Abu Dhabi, UAE.

S. Abdul Hadi, A. Nayfeh, Sueda Saylan, Marcus Dahlem are with MIST, Abu Dhabi, (e-mail:sabdulhadi@masdar.ac.ae; anayfeh@masdar.ac.ae).

T. Milakovich, M. T. Bulsara, E. A. Fitzgerald are with Massachusetts Institute of Technology, Cambridge, Massachusetts 02139, USA (e-mail: tmilakov@gmail.com; mayank.bulsara@gmail.com ; eafitz@mit.edu).

generated current limits current flow in tandem cell, decreasing its overall efficiency. Hence, ARC for Si based MJ cells should be designed to maximize optical absorption in Si base cell, but also not to impair performance of the top cell significantly.

In this paper we analyze the design requirements for $GaAs_{1-x}P_x$ /Si tandem cell for x= 0, 0.17, 0.29 and 0.37 in terms of optimum $GaAs_{1-x}P_x$ absorber layer thickness and single layer anti-reflective coating (SLARC). Analysis is carried out for 5 different ARC materials: Si_3N_4, SiO_2, ITO, HfO_2 and Al_2O_3, that were chosen either based on their optical compatibility with GaAsP, their common use in PV application or convenience of the in-situ growth. Transfer Matrix Method (TMM) is used to estimate the range of optimum anti-reflective layer thicknesses, which are then analyzed by optical and electrical simulations using TCAD Synopsys [20-22]. Finally, results for optimized $GaAs_{1-x}P_x$/Si tandem cell with optimum SLARC design is compared to the equivalent cell with optimized SiO_2/Si_3N_4 double layer anti-reflective coating (DLARC) [4,23].

II. METHODOLOGY

Various ARC materials were analyzed to observe how well they satisfy quarter-wave film condition. Transfer Matrix Method (TMM) is then used to estimate SLARC thickness, *d*, with minimum reflection for Air/ARC/$GaAs_{1-x}P_x$/Si interface with varying $GaAs_{1-x}P_x$ thickness, without taking into consideration the light absorption in each layer. In order to account for absorption and to find optimum ARC design for tandem cell, *d* is further varied in TCAD simulations. Moreover, $GaAs_{1-x}P_x$ layer thickness, *t*, is varied in order to find optimum tandem cell design with matching sub-cell currents. $GaAs_{1-x}P_x$ / Si tandem cell is simulated for top cell thickness, *t*, and ARC thickness, *d*, for varying $GaAs_{1-x}P_x$ minority carrier lifetime, τ, in order to find an optimum tandem cell design with maximum efficiency. Moreover, the efficiency of the tandem cell is used to identify the optimum design that can be achieved. The efficiency is a performance parameter that encapsulates effects of all variables in this analysis, such as ARC material, ARC thickness, $GaAs_{1-x}P_x$ absorber layer thickness and lifetime. Finally, by means of TCAD simulations, SiO_2/Si_3N_4 DLARC is optimized for the most efficient GaAsP/Si tandem cell and compared to optimum SLARC design.

A. *Selection of SLARC materials*

Quarter-wave films are specially designed to reduce or completely eliminate reflection at the interface between two media of different refractive indices, n. In our ARC selection process, quarter-wave (QW) condition was analyzed for Air (n_{Air}~1) / GaP (n_{GaP}~3) and Air / GaAs (n_{GaAs}~3.4) interfaces, as shown in equation (1) [24], since QW condition for $GaAs_{1-x}P_x$ compounds should fall in between.

$$n_{ARC} = \sqrt{n_{Air} \cdot n_{GaAs_{1-x}P_x}} \tag{1}$$

Figure 1 shows refractive indices of selected ARC materials, QW conditions for GaAs/Air and GaP/Air interfaces (optical properties utilized from [25]) and solar spectral irradiance AM1.5 [26]. Optical parameters of $GaAs_{1-x}P_x$ are obtained by measurements by J. A. Woollam Co. of MOCVD grown 2 μm thick $GaAs_{1-x}P_x$ layers on graded SiGe buffer [27]. In terms of reflection, SiO_2 performs poorly for the entire wavelength range and it is included in our further study due to its good surface passivation properties and DLARC applications [4, 23]. For wavelengths with highest spectral intensity (λ ~ 400-600 nm), Si_3N_4, ITO and HfO_2 satisfy QW condition for $GaAs_{1-x}P_x$ compounds the best, while Al_2O_3 is close to QW condition of Air/GaP interface.

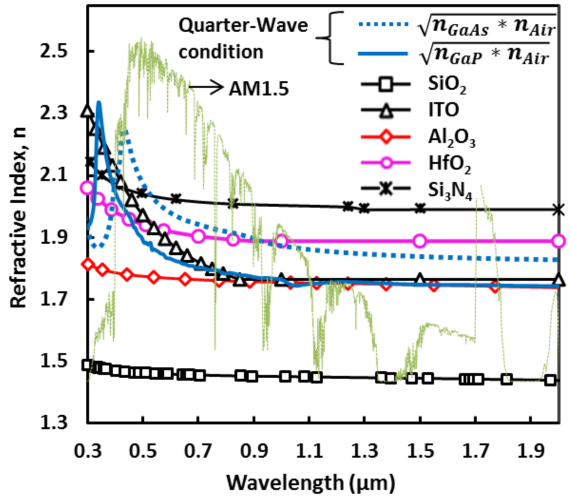

Fig.1. Refractive indices of analyzed ARC materials [25]. Also shown are quarter-wave conditions for Air/GaAs and Air/GaP interfaces as well as Solar Spectral Irradiance AM1.5(arbitrary units) [26].

B. *Transfer Matrix Method*

Transfer Matrix Method (TMM) is used to calculate the incident wave reflection with wavelength λ, propagating through multiple layers with refractive index n_i and thickness, d_i, without accounting for absorption in each medium. Wave transfer matrix used to describe propagation of the wave through homogenous i^{th} layer is defined in (2) and transfer matrix describing reflectance at the boundary of two layers with different refractive indices, n_i and n_{i+1} , is given in (3) [24].

$$M_{prop\_i} = \begin{bmatrix} e^{-j\varphi_i} & 0 \\ 0 & e^{j\varphi_i} \end{bmatrix}, \varphi_i = n_i d_i \frac{2\pi}{\lambda} \tag{2}$$

$$M_{i/i+1} = \frac{1}{2 \cdot n_{i+1}} \begin{bmatrix} n_{i+1} + n_i & n_{i+1} - n_i \\ n_{i+1} - n_i & n_{i+1} + n_i \end{bmatrix} \tag{3}$$

Wave propagating through N layers, assuming N+1 boundaries (sandwiched between two infinite media), can be described by matrix M, given in (4) [24].

$$M = \begin{bmatrix} A & B \\ C & D \end{bmatrix} = \prod_{i=1}^{N} (M_{i-1/i} \ M_{prop\_i} M_{i/i+1}) \tag{4}$$

Total intensity reflectance of wave propagation through N layers, from infinite region with n_0 to infinite region with n_{N+1} is then equal to [24]:

$$R_{0,N+1} = \left|-\frac{C}{D}\right|^2 \tag{5}$$

Figure 2 shows schematics of transfer matrix method applied to ARC optimization for $GaAs_{1-x}P_x$ / Si tandem cell.

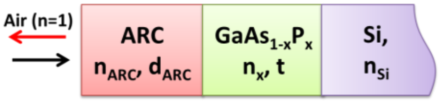

Fig. 2. Schematics of TMM structure used in order to estimate optimum ARC for $GaAs_{1-x}P_x$ / Si tandem cell.

In order to find optimum SLARC thickness, reflectance intensity at each wavelength, $R_{0,N+1}$ (λ), is weighted by normalized spectrum intensity, $I(\lambda)$, and averaged over the spectrum, as shown in (6).

$$R_{average} = \frac{1}{\lambda_{end}-\lambda_{start}} \int_{\lambda_{start}}^{\lambda_{end}} R_{0,N+1}(\lambda) \cdot I(\lambda) d\lambda \tag{6}$$

Solar spectrum range from λ_{start} = 300 nm to λ_{end} = 1100 nm is taken into consideration since $GaAs_{1-x}P_x$ and Si optical responsevity fall within it. Analysis is repeated for varying $GaAs_{1-x}P_x$ thickness and P fractions of x = 0, 0.17, 0.29 and 0.37. Figure 3 shows minimum average spectral weighted reflectance, $R_{average}$ as a function of P fraction (x), for each analyzed ARC material. $GaAs_{1-x}P_x$ thickness with minimum $R_{average}$ varied with x and was equal to 2, 0.8, 2 (1.3 for SiO_2) and 1 µm for x = 0, 0.17, 0.29 and 0.37 respectively.

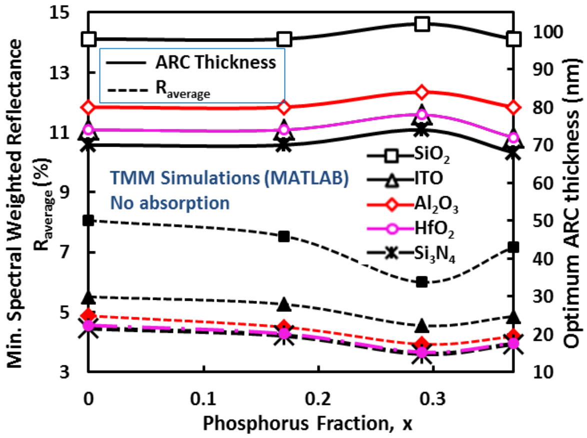

Fig. 3. Minimum average weighted reflectance, $R_{average}$ (%) as a function of P fraction, x, for different ARC material. $GaAs_{1-x}P_x$ thickness with minimum Raverage shown above is equal to 2, 0.8, 2 (1.3 for SiO_2) and 1 µm for x = 0, 0.17, 0.29 and 0.37 respectively.

When absorption is not taken into account, optimum ARC thickness ranges roughly between 65 to 85 nm for all tested fractions of x and ARC materials, with exception of SiO_2. HfO_2 and Si_3N_4 show the lowest reflectance over the analyzed spectrum range (3.6 %). Si_3N_4 requires least ARC thickness to achieve minimum reflectance and is closely followed by HfO_2.

SLARC thickness with minimum average reflectance over the entire solar spectrum is selected for further device simulations in TCAD.

C. TCAD Simulation Model

Sentaurus TCAD by Synopsys [20-22] is used for electrical and optical simulation of the solar cell devices. Synopsys tools Sentaurus Structure Editor (SDE), Sentaurus Device (SDevice) and Inspect are used.

$GaAs_{1-x}P_x$ / Si tandem cells are simulated for different ARC materials with varying ARC and $GaAs_{1-x}P_x$ thickness, as well as $GaAs_{1-x}P_x$ lifetime. Complex refractive indices for ARC materials, GaAs and Si are used from [25] while optical parameters of $GaAs_{1-x}P_x$ (x=0.17-0.37) are obtained by measurements of MOCVD grown 2 µm thick epi layer [27].

The Si solar cell is optimized such that absorber is 650 µm thick, lightly doped p-type Si substrate ($N_A=10^{16}$ cm^{-3}) and heavily doped ($N_D=10^{19}$ cm^{-3}) 100 nm thick n-type emitter. $GaAs_{1-x}P_x$ top cell is designed with variable absorber thickness and acceptor doping $N_A=10^{18}$ cm^{-3} and 50 nm thick emitter with $N_D=5x10^{18}$ cm^{-3}. Lifetime, τ, of Si is modeled as doping dependent in Physics section of SDevice Synopsys tool and its intrinsic value is set to 1 ms consistent with high quality c-Si wafer [28-30]. $GaAs_{1-x}P_x$ lifetime is modeled as fixed value and it is varied from 10 ps to 1 µs, range of values reported for GaAs epi growth on SiGe graded buffers [31] and pure GaAs materials [32]. Values for energy bandgap for $GaAs_{1-x}P_x$ are utilized from [33], while for Si and GaAs default values from TCAD are used. Tunnel diode between two cells is simulated as a very thin, highly conductive region [34]. Optical and resistive losses in tunnel junction are not taken into consideration in these simulations. Effect of interface surface recombination is also ignored. Figure 4 shows a schematic crossection of simulated solar cell.

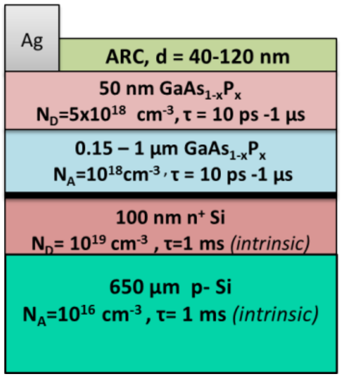

Fig. 4. Schematic cross-section of $GaAs_xP_{1-x}$ / Si tandem cell simulated in TCAD.

By increasing P fraction, the bandgap of the top $GaAs_{1-x}P_x$ cell increases from ~ 1.43 eV for x=0 to ~1.88 eV for x=0.37 [33] resulting in lower photogenerated current in the top cell. In order to achieve matching currents of subcells, the optimum $GaAs_{1-x}P_x$ absorber layer thickness, as well as optimum SLARC thickness changes with increasing P fraction. Consequently, optimum SLARC thickness and material will differ from the values estimated by TMM analysis that did not take into consideration the absorption or the tandem cell specific requirement for matching sub-cell currents.

III. RESULTS AND DISCUSSION

In order to show the effect of P fraction on the optimum SLARC and $GaAs_{1-x}P_x$ absorber layer thickness, TCAD simulations were carried out for Si_3N_4 as a fixed ARC material, based on TMM results (shown in Figure 3 earlier). Figure 5 (a) shows maximum efficiency of $GaAs_{1-x}P_x$/Si tandem cell as a function of $GaAs_{1-x}P_x$ absorber layer thickness at optimum Si_3N_4 ARC thickness for x=0, 0.17, 0.29 and 0.37, with $GaAs_{1-x}P_x$ lifetime τ=10 ns. $GaAs_{1-x}P_x$ absorber layer thickness for maximum efficiency increases from 250 nm for x = 0 to ~1 μm for x = 0.29 and 0.37. Tandem cell for x=0.29 preforms the best with maximum efficiency ~ 26.57%, closely followed by cells with x=0.37.

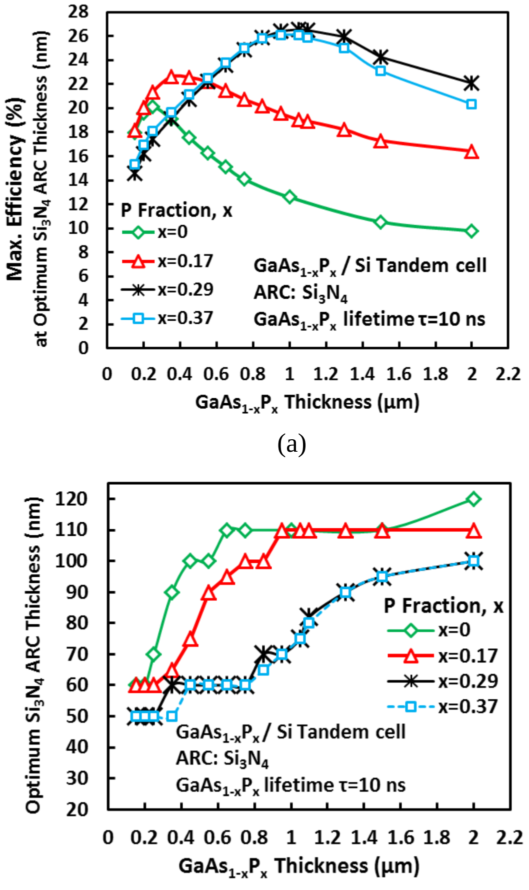

(a)

(b)

Fig. 5. (a) Maximum efficiency of $GaAs_{1-x}P_x$/Si tandem cell and (b) Optimum Si_3N_4 ARC thickness (nm) as a function of $GaAs_{1-x}P_x$ absorber layer thickness for x=0, 0.17, 0.29 and 0.37 and $GaAs_{1-x}P_x$ lifetime τ=10 ns.

Figure 5 (b) shows values for optimum Si_3N_4 ARC thickness at which maximum efficiency is achieved for varying $GaAs_{1-x}P_x$ absorber layer thickness and P fraction x. Maximum overall efficiency for all P fractions was achieved for Si_3N_4 thickness in the range between 65 – 75 nm. However, optimum ARC thickness increases with increasing $GaAs_{1-x}P_x$ absorber layer thickness. This is due to the fact that more light is absorbed in the top cell with thicker absorber layer and photogeneration in bottom Si cell needs to be enhanced by favoring longer wavelengths. Furthermore, the trend in Figure 5 (b) shows that generally thicker ARC layer is required for cells with lower P fraction (x=0 and 0.17). This is due to the fact that cells with lower bandgap absorb more of the solar spectrum so the ARC thickness needs to be tuned such that performance of bottom cell is maximized. Similar analysis was repeated for other ARC materials. Optimum ARC thickness as a function of P fraction (x), and its corresponding optimum $GaAs_{1-x}P_x$ absorber layer thickness for different ARC materials are shown in Figure 6 (a) for lifetime $GaAs_{1-x}P_x$ = 10 ns. Figure 6 (b) shows maximum efficiency as a function of P fraction for $GaAs_{1-x}P_x$ / Si tandem cells with optimized ARC and $GaAs_{1-x}P_x$ absorber layer thicknesses.

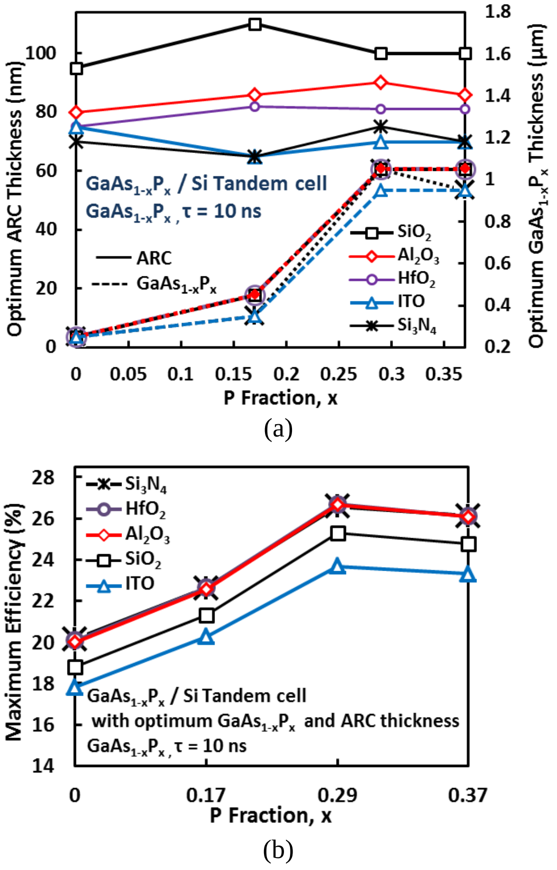

(a)

(b)

Fig.6. (a) Optimum SLARC thickness for optimum $GaAs_{1-x}P_x$ absorber layer thickness for different ARC materials and (b) maximum efficiency as a function of P fraction x for optimized $GaAs_{1-x}P_x$ / Si tandem cells with $GaAs_{1-x}P_x$ lifetime τ=10 ns.

Results in Figure 6 show that optimum SLARC thickness is smallest for Si_3N_4 and ITO (65 -75 nm) and largest for SiO_2 (~100-110 nm). Optimum top absorber thickness is mostly unchanged with respect to different ARC materials, with the exception of ITO that resulted in slightly thinner $GaAs_{1-x}P_x$ layer. In terms of efficiency, for all P concentrations, Si_3N_4, HfO_2 and Al_2O_3 performed almost equally, while SiO_2 and ITO resulted in ~1% and ~2% lower efficiency, respectively. With respect to ARC performance and optimum thickness, TCAD simulations are in agreement with TMM results (Figure 3) except for ITO that was outperformed by SiO_2. This is probably the result of larger absorption in ITO compared to SiO_2, due to its higher extinction coefficients, k [25].

We have shown that optimum SLARC thickness changes with changing $GaAs_{1-x}P_x$ absorber layer, due to the change in photogenerated current of both sub-cells. Similarly, optimum SLARC thickness changes with $GaAs_{1-x}P_x$ material quality, which in this work is represented by minority carrier lifetime, τ. Optimum SLARC and $GaAs_{1-x}P_x$ absorber layer thickness were studied for $10\ \text{ps} \leq \tau \leq 1\ \mu\text{s}$. Since x=0.29 resulted in highest efficiency (for $GaAs_{1-x}P_x$ absorber layer thickness between 950 nm – 1 μm), the effect of $GaAs_{1-x}P_x$ lifetime is shown here for that specific P fraction.

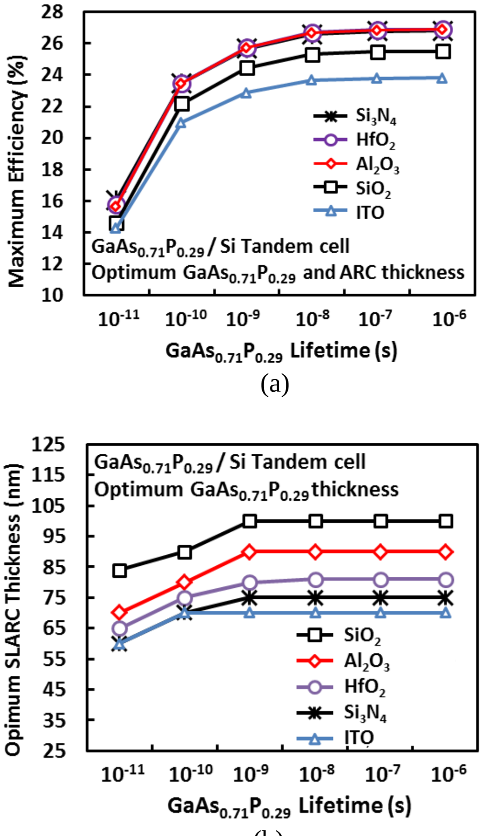

(a)

(b)

Figure 7 (a) Maximum efficiency and (b) optimum SLARC thickness as a function of $GaAs_{0.71}P_{0.29}$ minority carrier lifetime, τ, for $GaAs_{0.71}P_{0.29}$/ Si tandem cell with optimum $GaAs_{0.71}P_{0.29}$ absorber thickness.

Figure 7 (a) shows maximum efficiency of $GaAs_{0.71}P_{0.29}$ / Si tandem cell with optimized top cell absorber and ARC thicknesses, as a function of τ. The advantage of Si_3N_4, Al_2O_3 and HfO_2 materials decreases with lower material quality, with efficiency gain ranging from ~ 1.5 % at 10 ps to ~ 3% at 1 μs when compared with ITO. Figure 7 (b) shows optimum ARC thickness as a function of τ for $GaAs_{0.71}P_{0.29}$ / Si tandem cell with optimum top cell absorber thickness. Optimum ARC thickness increases as material quality of the top cell increases, in an attempt to enhance photogeneration in bottom cell. Similarly, for poor lifetime in top cells, ARC thickness decreases in favor of optical generation in top cell. The same trend is observed for all ARC materials and all P fractions (not shown here).

Figure 8 shows JV characteristics of $GaAs_{1-x}P_x$/Si tandem cells (x=0, 0.17, 0.29 and 0.37) with optimum SLARC and $GaAs_{1-x}P_x$ absorber layer thicknesses with $GaAs_{1-x}P_x$ lifetime equal to 10 ns. It can be noted that fill factor (FF) of cells with x=0.29 and x=0.37 is slightly higher, due to better match between subcell currents.

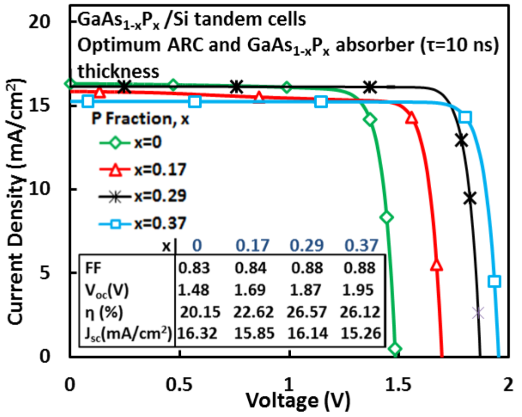

x	0	0.17	0.29	0.37
FF	0.83	0.84	0.88	0.88
V_{oc}(V)	1.48	1.69	1.87	1.95
η (%)	20.15	22.62	26.57	26.12
J_{sc}(mA/cm²)	16.32	15.85	16.14	15.26

Fig.8. JV characteristics of $GaAs_{1-x}P_x$/Si tandem cells (x=0, 0.17, 0.29 and 0.37) with optimum SLARC and $GaAs_{1-x}P_x$ absorber layer thicknesses with $GaAs_{1-x}P_x$ lifetime equal to 10 ns.

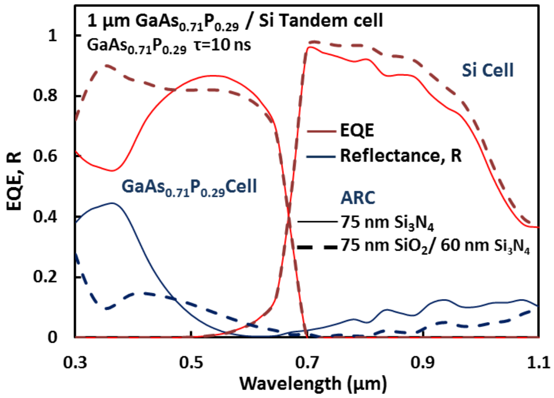

Fig.9. EQE (red) and Reflectance (blue) curves for 1 μm $GaAs_{0.71}P_{0.29}$ /Si tandem cell with 75 nm Si_3N_4 SLARC (full line) and 75 nm SiO_2 / 60 nm Si_3N_4 DLARC (dashed line). $GaAs_{0.71}P_{0.29}$ lifetime equals to 10 ns.

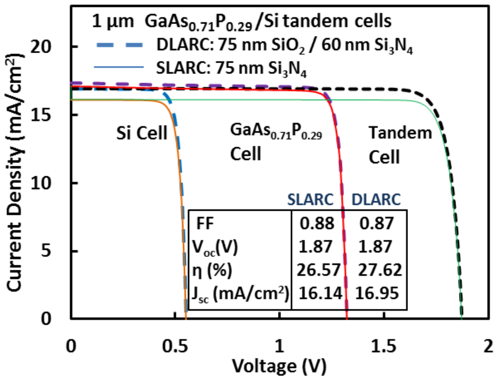

	SLARC	DLARC
FF	0.88	0.87
V_{oc}(V)	1.87	1.87
η (%)	26.57	27.62
J_{sc} (mA/cm²)	16.14	16.95

Fig.10. JV characteristics $GaAs_{0.71}P_{0.29}$/Si of top, bottom and tandem cell for 75 nm Si_3N_4 SLARC (full lines) and 75 nm SiO_2 / 60 nm Si_3N_4 DLARC (dashed lines). $GaAs_{0.71}P_{0.29}$ lifetime equals to 10 ns.

Best preforming cell, with 1 µm thick GaAs$_{0.71}$P$_{0.29}$ absorber, is further improved by using optimized 75 nm SiO$_2$/ 60 nm Si$_3$N$_4$ DLARC. Figure 9 shows comparison of reflectance and External Quantum Efficiency (EQE) for 1 µm thick GaAs$_{0.71}$P$_{0.29}$ /Si tandem cell with 75 nm Si$_3$N$_4$ SLARC and 75 nm SiO$_2$ / 60 nm Si$_3$N4 DLARC. By using optimized SiO$_2$/Si$_3$N$_4$ DLARC overall reflectance is decreased, (for λ = 300-450 nm and $\lambda > 700$ nm). This results in improved spectral response of both cells, resulting in higher J$_{sc}$ and ~1% efficiency gain, as shown in Figure 10.

IV. CONCLUSION

In summary, a simulation study was carried out in order to find the optimum ARC material and thickness for GaAs$_{1-x}$P$_x$/Si tandem cells. Optimum SLARC thickness is smallest for Si$_3$N$_4$ and ITO (65 -75 nm) and largest for SiO$_2$ (~100-110 nm). However optimum ARC thickness increased with increasing GaAs$_{1-x}$P$_x$ absorber layer thickness. Furthermore, thicker ARC layer is required for cells with lower P fraction (x=0 and 0.17). The optimum GaAs$_{1-x}$P$_x$ absorber layer thickness increases from 250 nm for x = 0 to ~1 µm for x = 0.29 and 0.37. Maximum efficiency ~ 26.57% was achieved for cells with x=0.29 with optimized SLARC (75 nm Si$_3$N$_4$) and absorber layer thickness (~1 µm). For all P fractions, maximum efficiency was achieved for 65 – 75 nm thick Si$_3$N$_4$ SLARC. Finally, efficiency for ~1 µm GaAs$_{0.71}$P$_{0.29}$ /Si tandem cell is increased to 27.62 % by using optimized 75 nm SiO$_2$ / 60 nm Si$_3$N4 DLARC.

REFERENCES

[1] Y. Matsumoto, J. A. Urbano, M. Ortega, E. Barrera, G. Romero-Paredes, “Towards cost-effective antireflective-coating and surface-texturing”, *38th IEEE PVSC*, Austin, TX , 2012,, pp. 000258 - 000264

[2] J. Zhao, A. Wang, X. Dai, M.A. Green and S.R. Wenham, “Improvements in silicon solar cell performance”, in *22nd IEEE PVSC*, Las Vegas, NV, 1991, pp. 399 – 402.

[3] A. Al-Bustani, M.Y. Feteha, “Design of antireflection coatings for triple heterojunction AlGaAs-GaAs space solar cells”, *IEEE Workshop on High Performance Electron Devices for Microwave and Optoelectronic Applications*, 1995, pp. 55 – 60.

[4] K.A. Abade, , F.J. Fonseca, R.D. Mansano, P., Jr., Abade, “PECVD single-layer (SiN:H) and double-layer (SiN:H/SiO$_2$) ARC on mono and multicrystalline silicon solar cells“ *IEEE PVSC*, 2000, pp. 307-310.

[5] D. N. Wright, E. S. Marstein, A. Holt, “Double layer anti-reflective coatings for silicon solar cells”, *31st IEEE PVSC*, 2005, pp. 1237- 1240.

[6] M. Neander, F. Gromball, D. Neumann, N.P. Harder, W. A. Nositschka, “Anti-Reflective-Coating Tuned for Higher Solar Module Voltage”, *IEEE 4th World Conference on Photovoltaic Energy Conversion*, 2006, pp. 2070 - 2072.

[7] D. Bouhafsa, A. Moussia, A. Chikouchea, J.M. Ruizb (1998, March). Design and simulation of antireflection coating systems for optoelectronic devices: Application to silicon solar cells. *Solar Energy Materials and Solar Cells, 52(1–2)*, pp. 79–93.

[8] S.R. Kurtz, P. Faine, and J.M. Olson, "Modeling of two-junction, series-connected tandem solar cells using top-cell thickness as an adjustable parameter, *J. Appl. Phys. 68*, 1990, pp. 1890.

[9] J. A. Carlin, M. K. Hudait, S. A. Ringel, D. M. Wilt, E. B. Clark, C. W. Leitz, M. Currie, T. Langdo, and E. A. Fitzgerald, “High efficiency GaAs-on-Si solar cells with high V$_{oc}$ using graded GeSi Buffers,” in Proc. 28th IEEE Photovoltaics Spec. Conf., 2000, pp. 1006–1011.

[10] C. L. Andre, D. M. Wilt, A. J. Pitera, M. L. Lee, E. A. Fitzgerald, and S. A. Ringel, “Impact of dislocation densities on n+/p and p+/n junction GaAs diodes and solar cells on SiGe virtual substrates,” *J. Appl. Phys.*, vol. 98, no. 1, 2005, pp. 014502-1–014502-5.

[11] A. Nayfeh, “Heteroepitaxial growth of relaxed germanium on silicon,” Ph.D. thesis, Stanford University (2006).

[12] Ali K Okyay, M Cengiz Onbasli, Burcu Ercan, Hyun-Yong Yu, Shen Ren, David AB Miller, Krishna C Saraswat, and Ammar M Nayfeh, "High efficiency monolithic photodetectors for integrated optoelectronics in the near infrared", IEEE LEOS Annual Meeting Conference Proceedings, LEOS'09. pp. 303-304 October 4, 2009

[13] S. Abdul Hadi, P. Hashemi, N. DiLello, A. Nayfeh, J. L. Hoyt , “Effect of c-Si$_{1-x}$Ge$_x$ Thickness Grown by LPCVD on the Performance of Thin-Film a-Si/c-Si$_{1-x}$Ge$_x$/c-Si Heterojunction Solar Cells”, *MRS Proceedings*, 1447, mrss12-1447-v01-09, 2012.

[14] S. Abdul Hadi, P. Hashemi, N. DiLello, A. Nayfeh, J. L. Hoyt , “Thin film a-Si/c-Si$_{1-x}$Ge$_x$/c-Si heterojunction solar cells with Ge content up to 56%”, 38th IEEE PVSC, 2012, pp. 5-8.

[15] S. Abdul Hadi, P. Hashemi, N. DiLello, E. Polyzoeva, A.Nayfeh, J.L. Hoyt, “Thin-film Si$_{1-x}$Ge$_x$ HIT solar cells”, *Solar Energy*, vol. 103, May 2014, pp. 154–159

[16] K. Hayashi, T. Soga, H. Nishikawa, T. Jimbo and M. Umeno , “MOCVD growth of GaAsP on Si for tandem solar cell applications”, 1st World Conf. on Photovoltaic Energy Conversion, 1994, pp. 1890-1893.

[17] J.F. Geisz, J.M. Olson, M.J. Romero, C.S. Jiang, A.G. Norman, “Lattice-mismatched GaAsP Solar Cells Grown on Silicon by OMVPE”, 4th World Conf. on PV Energy Conversion, IEEE, 2006, pp. 772 – 775.

[18] T. J. Grassman, J.A. Carlin, S. D. Carnevale, I. Al Mansouri, H. Mehrvarz, S. Bremner, A. Ho-Baillie, E. García-Tabarés, I. Rey-Stolle, M. A. Green, S. A. Ringel, “Progress Toward a Si-Plus Architecture: Epitaxially-Integrable Si Sub-Cells for III-V/Si Multijunction Photovoltaics”, 40th IEEE PVSC, 2014.

[19] K. N. Yaung, J. R. Lang, M. L. Lee, “Towards high efficiency GaAsP solar cells on (001) GaP/Si”, 40th IEEE PVSC, 2014.

[20] TCAD: Process and device Simulation Tools, World Wide Web: http://www.synopsys.com/Tools/TCAD/Pages/default.aspx

[21] S. Abdul Hadi, A. Nayfeh, P. Hashemi, J. L. Hoyt “a-Si/c-Si$_{1-x}$Ge$_x$/c-Si heterojunction solar cells”, *SISPAD*, 2011, pp. 191-194.

[22] S. Abdul Hadi, P. Hashemi, A. Nayfeh, J. L. Hoyt, “Thin Film a-Si/c-Si$_{1-x}$Ge$_x$/c-Si Heterojunction Solar Cells: Design and Material Quality Requirements”, *ECS Transactions 41 (4),* 2011, pp. 3-14.

[23] B. Conrad, T. Zhang, A. Lochtefeld, A. Gerger, C. Ebert, M. Diaz, L. Wang, I. Perez-Wurfl, and A. Barnett, “Double Layer Antireflection Coating and Window Optimization for GaAsP/SiGe Tandem on Si”, 40th IEEE PVSC, 2014.

[24] B.E.A. Saleh and M.C. Teich, “Photonic-Crystal Optics” in *Fundamentals of Photonics*, 2nd ed. New Jersey, WILEY, 2007, ch. *7, sec. 1*, pp. 246-252.

[25] Sopra Semilab “n-k Database”, Web: http://www.sopra-sa.com.

[26] Reference Solar Spectral Irradiance Air Mass AM1.5, Avalable at: http://rredc.nrel.gov/solar/spectra/am1.5/

[27] Optical properties of MOCVD grown GaAs$_{1-x}$P$_x$ epi layers on SiGe graded buffers (to be published).

[28] J. E. Park, D. K. Schroder, S. E. Tan, B. D. Choi, M. Fletcher,A. Buczkowski, and F. Kirscht, “Silicon Epitaxial Layer Lifetime Characterization”, *Journal of The Electrocheical Society, 148(8)* G411-G419 (2001).

[29] A. Nayfeh, V. Koldyaev, P. Beaud, M. Nagoga, and S. Okhonin, IEEE SOI Conference Proceedings, 75 (2008).

[30] S. Abdul Hadi, P. Hashemi, N. DiLello, E. Polyzoeva, A. Nayfeh, J.L. Hoyt, “Effect of germanium fraction on the effective minority carrier lifetime in thin film amorphous-Si/crystalline-Si$_{1-x}$Ge$_x$/crystalline-Si heterojunction solar cells”, *AIP Advances 3 (5)*, 2013, pp. 052119-052119-6

[31] C. L. Andre, J. J. Boeckl, D. M. Wilt, A. J. Pitera, M. L. Lee, E. A. Fitzgerald, B. M. Keyes, S. A. Ringel, “Impact of dislocations on minority carrier electron and hole lifetimes in GaAs grown on metamorphic SiGe substrates”, *Applied Physics Letters, 84(18)*, 2004.

[32] Properties of GaAs. Available at: http://www.ioffe.ru/SVA/NSM/Semicond/GaAs/electric.html

[33] G. D. Pitt and C. E. E. Stewart, “The electrical properties of GaAs$_{1-x}$P$_x$ alloys from a high-pressure experiment”, J. Phys. C: Solid State Phys., Vol. 8, 1975.

[34] *Simulation of a GaAs/GaInP Dual-Junction Solar Cell*, Synopsys Inc., 2012. Available at https://solvnet.synopsys.com.